

BUREAU INTERNATIONAL DES POIDS ET MESURES

The SIRTI : a new tool developed at the BIPM for comparing activity measurements of short-lived radionuclides world-wide

C. Michotte, M. Nonis, C. Bobin, T. Altizoglou, G. Sibbens



2013

Pavillon de Breteuil, F-92312 SÈVRES Cedex, France

The SIRTI: a new tool developed at the BIPM for comparing activity measurements of short-lived radionuclides world-wide

C. Michotte*, M. Nonis*, C. Bobin[§], T. Altizoglou[#], G. Sibbens[#]

*BIPM, Bureau International des Poids et Mesures, Sèvres, France

[§]LNE-LNHB, Laboratoire National de Métrologie et d'Essais – Laboratoire National Henri Becquerel, CEA, Saclay, France

[#]IRMM, European Commission, Directorate General, Joint Research Centre, Institute for Reference Materials and Measurements, Retieseweg 111, B-2440 Geel, Belgium

For short-lived radionuclides, NMIs situated far from the BIPM are unable to participate in the BIPM.RI(II)-K1 comparisons by sending samples to the SIR. Consequently, a Transfer Instrument (SIRTI) based on a transportable well-type NaI(Tl) detector calibrated against the SIR for ^{99m}Tc has been developed at the BIPM and is the basis of the BIPM.RI(II)-K4 comparison. Full details of this new system and the tests carried out are reported. Uncertainties are discussed.

Introduction

Short-lived radionuclides are essential for nuclear medicine and radionuclides with half-lives much shorter than one day are used as radiotracers. The use of nuclear medicine is increasing as these radionuclides become more accessible and they attract the interest of the National Metrology Institutes (NMIs). However, as a consequence of the short half-lives, sending ampoules that contain such radioactive material to the Bureau International des Poids et Mesures (BIPM) for activity measurement of γ -ray-emitting radionuclides in the International Reference System (SIR) is only practical for NMIs that are based in Europe. In order to extend the use of the SIR and to enable other NMIs to participate, a transfer instrument (SIRTI) has been developed at the BIPM following a request by the CCRI(II) in 2005 and with the support of the Consultative Committee for Ionizing Radiation CCRI(II) Transfer Instrument Working Group [1, 2]. The SIRTI was calibrated against the SIR which enabled comparison of results in the SIRTI comparison with those in the SIR.

The choice of a NaI(Tl) crystal as the transfer instrument has been described in [1]. Other choices were proposed (ionization chamber [1] or plastic scintillator [3]) but were not used in the final design. Full details of this new system (the detector, mechanical parts and associated electronics) and all the tests carried out are reported. Uncertainties are discussed.

1. Description of the SIRTI (Figure 1)

The detector is a well-type 3" × 3" NaI(Tl) crystal from Saint-Gobain Crystals (France). The well designed to hold the SIR-type ampoule is 5 cm deep and 2 cm in diameter. The crystal is coupled with an ETL 9305 photomultiplier. The detector is supported by a tripod which was designed and constructed in the BIPM workshop, using an aluminium clamping annulus (indicated by the letter A in Figure 1) and layers of aluminium tape for adjustments during tightening. The verticality of the detector can be adjusted using three pushing/pulling horizontal screws (indicated by the letter S).

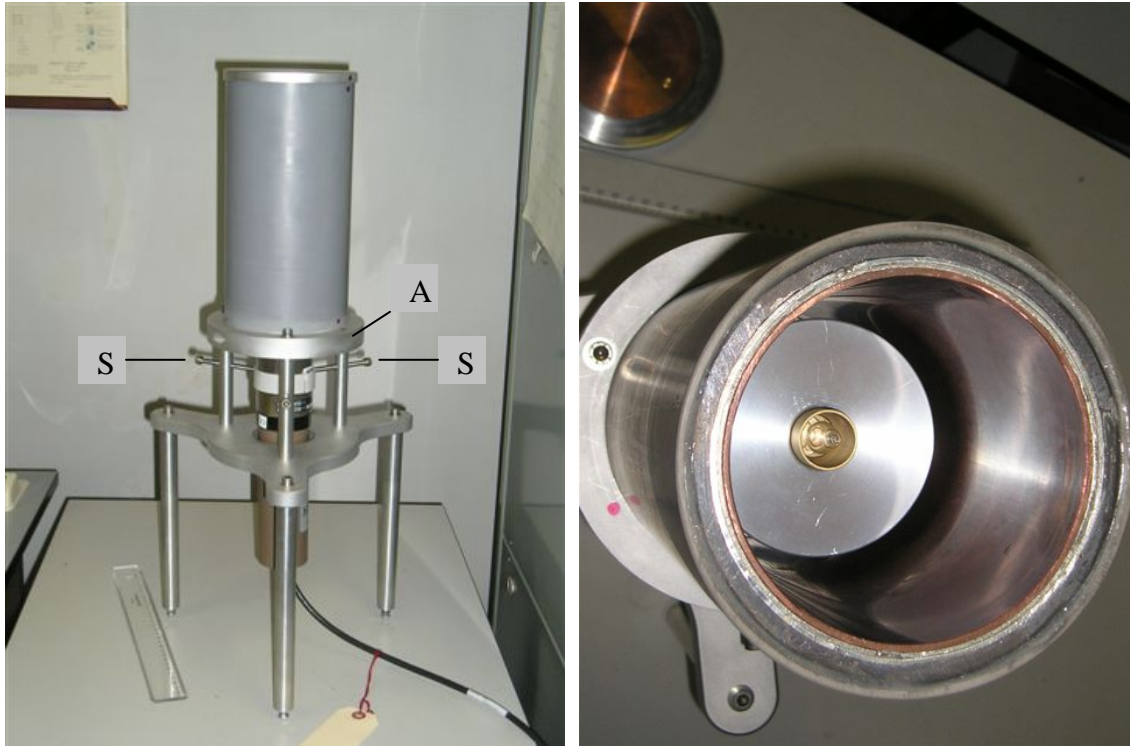


Figure 1. The SIRT on its tripod and surrounded by the graded shielding. An SIR ampoule can be seen in a brass liner in the well. See text for more information.

The detector is surrounded by a thin graded shielding (5 mm of Pb, 3 mm of Sn, 2 mm of Cu) fixed in a protective PVC tube using adhesive. The shielding stands on the tripod without binding. Additional binding is necessary for comparisons in countries with a high risk of seismological activity for security reasons. The shielding is necessary to reduce the natural background and the influence of backscattering on the surroundings. The background count rates with and without the shielding are around 70 s^{-1} and 300 s^{-1} respectively. The shielding reduces mainly the low energy part of the background spectrum as shown in Figure 2.

When transporting the detector to the participants, care should be taken to protect the detector from temperature changes of greater than $8 \text{ }^{\circ}\text{C}$ per hour which could damage the

crystal. A single layer of thermal insulating sheet around the case has proved to be sufficient.

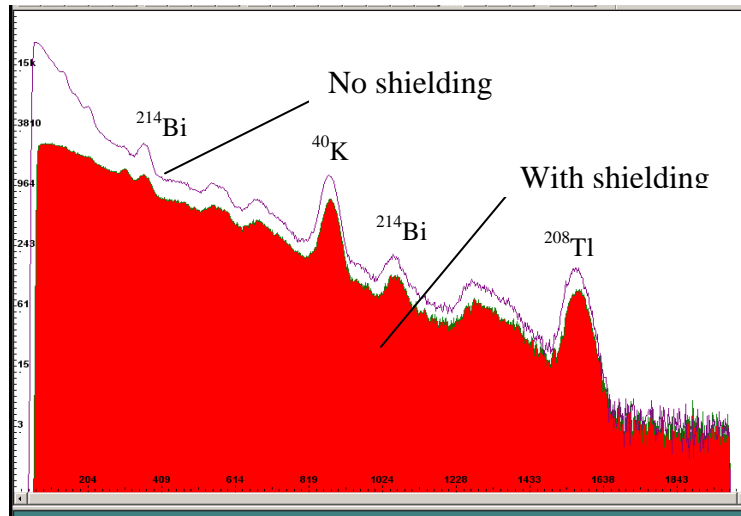


Figure 2. Background energy spectrum of the SIRTl with and without shielding.

The reference source (see section 2) is an irradiated wire (1 mm long and 0.2 mm diameter), donated by the IRMM, which contains both the ^{94}Nb and the $^{93\text{m}}\text{Nb}$ isotopes. Its Plexiglass holder has been designed to be dismantable and uses the minimum material possible in order to minimize the absorption of the $^{93\text{m}}\text{Nb}$ x-rays (see Figure 3 and Annex 1).

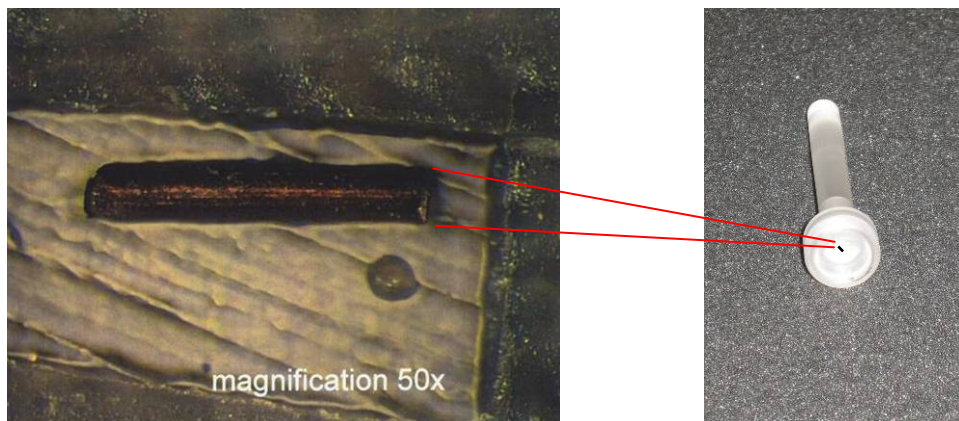


Figure 3. Nb reference source and its Plexiglass holder

A cylindrical x-ray liner closed at the bottom has been machined from a single piece of brass in the BIPM workshop (see Annex 2). The chemical composition of the brass was selected carefully to avoid high Z elements that could emit high-energy fluorescence x-rays. The internal bottom surface is not uniform and was hollowed-out to a depth of 0.5 mm to avoid difficulties in reproducibility of the ampoule position. The wall thickness of the brass liner is between 1 mm (top) and 2 mm (bottom). Two backup copies of the liner

were produced and their thickness adjusted (0.01 mm at a time) in order to have identical count rates in the SIRT I for an ampoule containing ^{57}Co , used to simulate $^{99\text{m}}\text{Tc}$ (Table 1).

	Brass 1	Brass 2	Brass 3
^{57}Co count rate / s^{-1}	25 065 (23)	25 072 (20)	25 070 (16)

Table 1: Count rate of the ^{57}Co source with the 3 different liners.

2. Measurement principle

The measurand is the $^{99\text{m}}\text{Tc}$ count rate above a low-energy threshold, relative to the ^{94}Nb count rate above the same threshold. The threshold energy is adjusted by using the $^{93\text{m}}\text{Nb}$ x-ray peak at 16.6 keV.

The stability of the SIRT I is monitored using the ^{94}Nb reference source ($T_{1/2} = 20\,300$ (1 600) a [4]). Once the threshold is set, the brass liner is placed in the well to suppress the $^{93\text{m}}\text{Nb}$ contribution to the ^{94}Nb stability measurements. Niobium-93m could not be used for the long-term stability checks due to its short half-life and because it has a peak close to the threshold which makes the measurement highly sensitive to fluctuations in the threshold level.

The $^{99\text{m}}\text{Tc}$ SIR ampoules are also placed in the detector well with the brass liner to suppress the contribution of $^{99\text{m}}\text{Tc}$ x-ray peaks at 18.4 keV to the count rate (detection efficiency lower than 10^{-5}), making the measurements much less sensitive to the threshold position. No extrapolation to zero energy is carried out as all the measurements are made with the same threshold setting and because the objective is not to make a primary measurement but to compare measurements made at different NMIs under the same conditions.

A SIRT I equivalent activity A_E is deduced from the $^{99\text{m}}\text{Tc}$ and ^{94}Nb counting results and the $^{99\text{m}}\text{Tc}$ activity A measured by the NMI. The presence of ^{99}Mo in the solution should normally be accounted for using γ -spectrometry measurements carried out by the NMI.

$$A_E = A \frac{c_1}{\lambda_{\text{Tc}}} \frac{\rho_{\text{Nb}}}{N} \left[1 + R \frac{\varepsilon_{\text{Mo}}}{\varepsilon_{\text{Tc}}} \frac{\lambda_{\text{Tc}}}{\lambda_{\text{Mo}}} \frac{c_2}{c_1} + BR \frac{\lambda_{\text{Tc}}}{c_1} \left(\frac{\lambda_{\text{Tc}} c_2 - \lambda_{\text{Mo}} c_1}{\lambda_{\text{Mo}} (\lambda_{\text{Tc}} - \lambda_{\text{Mo}})} \right) \right] \quad (1)$$

$$c_1 = \left(e^{-\lambda_{\text{Tc}} t_i} - e^{-\lambda_{\text{Tc}} (t_i + \Delta t)} \right) / e^{-\lambda_{\text{Tc}} t_R}$$

$$c_2 = \left(e^{-\lambda_{\text{Mo}} t_i} - e^{-\lambda_{\text{Mo}} (t_i + \Delta t)} \right) / e^{-\lambda_{\text{Mo}} t_R}$$

with	A	^{99m}Tc activity at the reference time t_R
	R	^{99}Mo to ^{99m}Tc activity ratio
	$B = 0.876$ (19)	branching ratio of production of ^{99m}Tc in the ^{99}Mo decay
	N	^{99m}Tc counting corrected for live time and background
	ρ_{Nb}	count rate of the ^{94}Nb measurement corrected for live time and background and calculated at $t = 1$ March 2007
	ε_{Tc} and ε_{Mo}	SIRTI detection efficiency for ^{99m}Tc and ^{99}Mo (without ^{99m}Tc) respectively
	λ_{Tc} and λ_{Mo}	decay constant of ^{99m}Tc and ^{99}Mo respectively
	c_1 and c_2	decay correction for ^{99m}Tc and ^{99}Mo (without ^{99m}Tc) respectively
	t_i	time of the beginning of the measurement
	Δt	measurement duration.

The second term in the square brackets corresponds to the contribution of ^{99}Mo while the third term is the ^{99m}Tc growth from the ^{99}Mo decay. The detection efficiency of the SIRTI for ^{99}Mo ε_{Mo} has been measured at the BIPM using ^{99}Mo solutions in SIR ampoules provided by the NIST and the LNE-LNHB [5]. The detection efficiency ε_{Tc} is deduced from ^{99m}Tc measurements with negligible ^{99}Mo content, in which case

$$\varepsilon_{\text{Tc}}^{-1} = \frac{A}{N} \frac{c_1}{\lambda_{\text{Tc}}}$$

The use of ^{94}Nb for the stability checks may be not the best choice because the emitted gamma-rays have an energy that is more than five times higher than ^{99m}Tc . However, if for any reason the stability of the system is questioned, the SIRTI can easily be re-calibrated against the SIR and a new series of stability checks restarted.

3. Electronics: description and tests (Figure 4)

The NaI(Tl) crystal is coupled to an ETI9305KFLB02 photomultiplier tube, supplied by an ORTEC 296 Scintipack base and preamplifier. The high voltage supplied is 900 V and the preamplifier gain is one. The ORTEC 590A amplifier is then used in connection with the pocket ADMCA 8000A ADC and multichannel analyser from AMPTEK (USA) with 2048 channels. The unipolar pulses from the amplifier have a shaping of 0.5 μs . The range of the ADMCA is set to 5 V in order to enlarge the low energy part of the spectrum without further increasing the amplifier gain which would have increased the rate of saturating pulses.

The energy resolution expressed by the Full Width at Half Maximum (FWHM), as measured at reception of the detector, complies with the manufacturer's specifications and is given in Table 2. These values, given by the ADMCA software, are only

indicative. Indeed they depend on the selected region of interest and its centroid which may differ significantly from the peak position especially for asymmetrical peaks.

Energy / keV	FWHM / %	Comment
23 keV (^{109}Cd)	25	Range MCA 10 V; amp. gain $\times 2$
88 keV (^{109}Cd)	11	Range MCA 10 V; amp. gain $\times 2$
130 keV (^{57}Co)	10	Range MCA 10 V
165 keV (^{139}Ce)	9	Range MCA 10 V
662 keV (^{137}Cs)	6.5	Range MCA 10 V; amp. gain $\times 0.5$ Source outside the well

Table 2: FWHM energy resolution at reception of the detector

3.1 Live-time module

As the live-time correction provided by an MCA is not sufficiently reliable especially at high count rate, a donated live-time module, the *Module de Temps mort Reconductible* (MTR2) designed at the LNE-LNHB [6], is used. The MTR2 has been slightly modified at the BIPM to decrease the minimal energy threshold, to change the range of dead time and, in June 2010, to make the threshold potentiometer more sensitive. The output counts from the MTR2 are counted by an ORTEC 994 scaler on one hand and are used to gate the MCA through a Gate and Delay generator ORTEC 416A on the other hand (see Figure 4). Gating the MCA by the MTR2 output counts enables the MTR2 threshold to be set at the position of the $^{93\text{m}}\text{Nb}$ x-ray peak identified in the MCA energy spectrum. The negative threshold of the MTR2 is set to the minimum while it remains higher than the electronic noise.

The live-time is measured using a 1 MHz oscillator or clock of known frequency f and by counting the survival clock's pulses C with the ORTEC scaler:

$$\rho = R / \left(\frac{C/T}{f} - Rdt \right)$$

where T is the measurement duration in seconds (real time), R the observed count rate, ρ the count rate corrected for dead-time losses and $dt = 5$ ns is the clock pulse width [7]. In fact, the TTL pulses from the clock are 500 ns wide but they are reshaped to 5 ns wide pulses by the MTR2. The frequency was selected to be at least ten times the maximum count rate. This ensures a negligible effect from the finite clock frequency on the live-time correction uncertainty [8].

The value of the extendable dead-time of the MTR2 has been adjusted to 30 μs . A long dead time is required to cover the wide saturating pulses followed by long undershoots, produced by high-energy gamma rays. Figure 5 shows that above 15 μs , the count rate corrected for dead time is independent of the dead-time value. The origin of the bias that appeared for low dead-time values and high count rate has been identified in the electronics of the MTR2 by the LNE-LNHB and has subsequently been corrected.

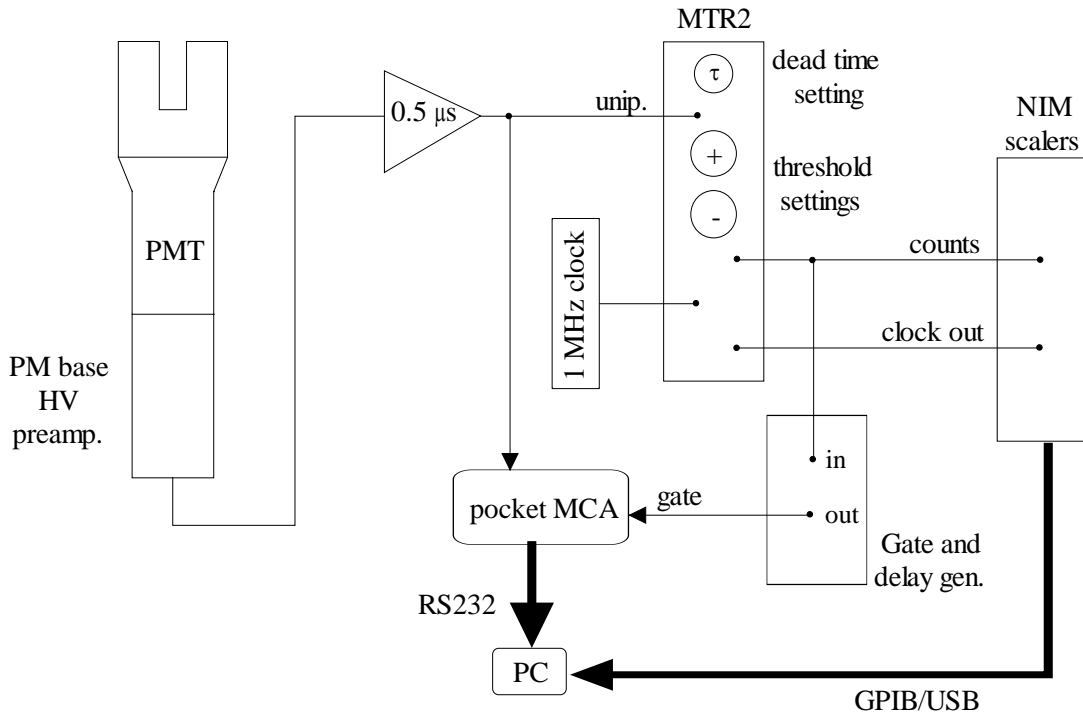


Figure 4: Block diagram of the SIRT1.

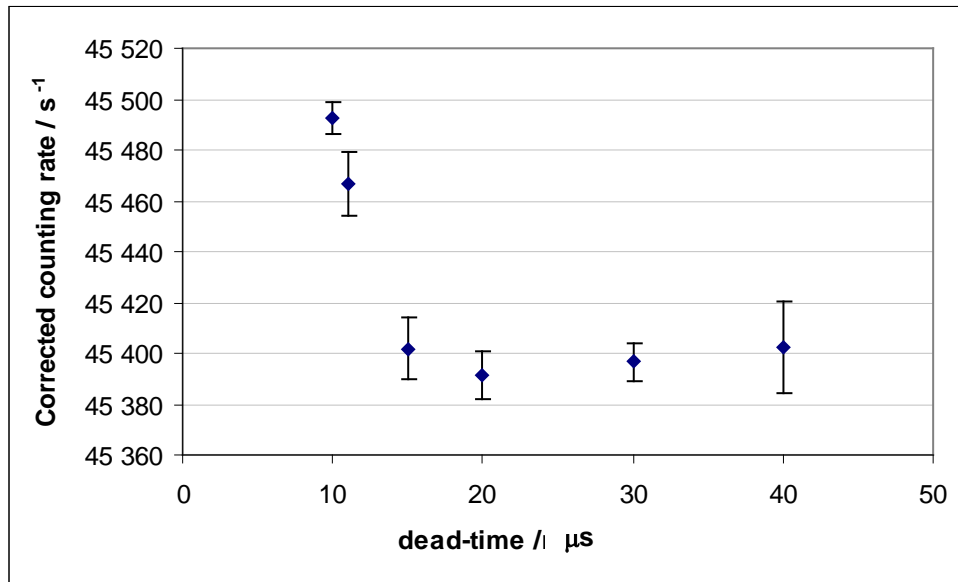


Figure 5: Influence of the MTR2 dead-time value on the count rate (^{154}Eu) corrected for dead time.

3.2 Scalers

The ORTEC 994 scalers are connected to a laptop through a GPIB/USB controller¹ and the counts are read using an interface program written in LabView8.2. The LabView interface is used to start the measurements and read the results while the measurement duration is controlled by the scaler internal time base. At the start of a measurement, LabView also reads the time from the laptop (using the function “Timestamp”) which is synchronized regularly with a NTP time server. When counting the clock pulses, the scaler overflow at 10^8 is rapidly reached. The overflows are detected and counted by checking on-line with LabView when $N(t + \Delta t) < N(t)$. It has been found that on occasions an overflow is not counted or an extra non-real overflow is counted. The reasons are not known, but this should not cause errors in the measurement results because a lack of or an extra 10^8 counts are easy to identify. Nevertheless, the replacement of the ORTEC scalers by National Instrument counters/timers (NI USB 6341) is planned.

The repeatability and accuracy of the ORTEC scalers and the LabView interface were extensively tested in 2006 by counting a 10 MHz frequency originating from an atomic clock traceable to the SI. The observed readings differed from the atomic frequency by 8×10^{-6} at a maximum (in relative terms), which complies with the typical frequency precision and stability of a quartz oscillator. When using a second ORTEC scaler, which was purchased later, the difference with the atomic clock frequency is 1.1×10^{-5} , a figure which is also compliant. In addition, the numbers of counts obtained are identical when counting the 10 MHz frequency in parallel on channels A and B of the scalers.

3.3 Live-time clock

The clock was constructed at the BIPM and is based on a TTL 5V 1 MHz quartz oscillator F1100ELF. The possibility to select a lower clock frequency with a jumper has been included using a programmable logic device. The frequency of the live-time clock has been measured using the ORTEC scalers and has been monitored since 2007 (see Figure 6). The results reflect the combined stability of the clock and the scalers. No reason could be identified to explain the low frequency measurement at the NIM, China, in March 2012. Nevertheless, such a change of the measured live-time clock frequency of 2×10^{-5} in relative terms has a negligible effect on the SIRTI comparison results. The monitoring clock measurements are supplemented by regular checks of the scalers' time base by counting the 10 MHz frequency traceable to the SI. Finally, it has been observed that the measured live-time clock frequency depends on temperature with a sensitivity coefficient of approximately 2 Hz per °C. This effect has a negligible effect on the comparison results.

¹ Type of controller no more supported by ORTEC and replaced by RS232

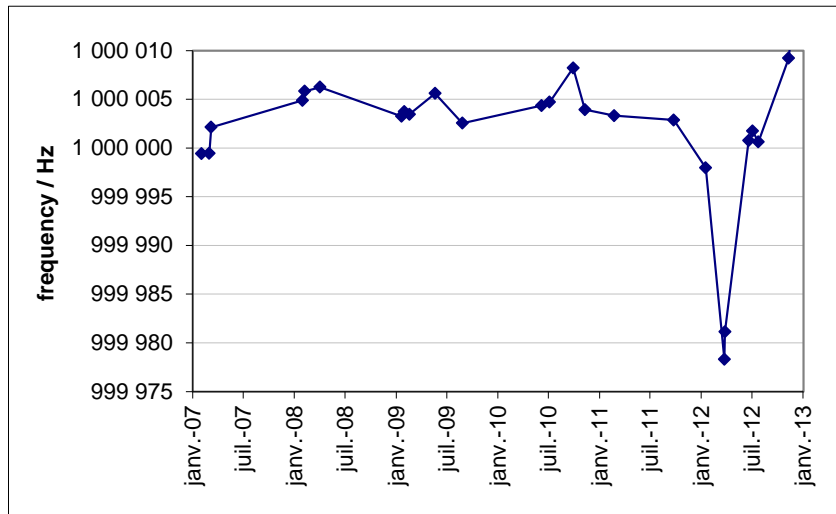


Figure 6. Stability measurements of the live-time clock and the scalers

3.4 Threshold stability

The response of a NaI(Tl) detector is known to be sensitive to temperature. Indeed the $^{93\text{m}}\text{Nb}$ x-ray peak position, used to define the threshold, shows dependence versus temperature equal to about -2 channels/ $^{\circ}\text{C}$. Shifts of 3 channels at maximum over 24 h periods were observed for the threshold position, around channel 100, in an air-conditioned laboratory at the BIPM.

The influence of such shifts on the measured count rate was quantified by measuring the count rate as a function of the threshold position in channels. The results consist in sensitivity coefficients of 8.8×10^{-5} per channel for ^{94}Nb and $< 10^{-5}$ per channel for ^{57}Co (see Figure 7). This means that for the ^{94}Nb measurements, a change of threshold position by a few channels can produce a non-negligible effect. It is thus important to check the threshold position (using the $^{93}\text{Nb}^{\text{m}}$ x-ray peak) before each ^{94}Nb measurement. For a radionuclide such as ^{57}Co (and $^{99\text{m}}\text{Tc}$ with the liner) where most counts are concentrated in the photopeak, the threshold position is not crucial and gain shifts during a long series of measurements (over 20 hours) should not affect the results.

3.5 Influence of the count rate

In view of the fact that the change of response of a NaI(Tl) measurement system as a function of the count rate is a known effect, investigations were carried out for the SIRTl. The stability of the energy spectrum as a function of the count rate has been studied. Measurements with a series of ^{57}Co sources with a large range of activity values showed that above a count rate of about $60\,000\text{ s}^{-1}$, peak shifts start to be significant (see Figure 8). The same behaviour with approximately the same slope was observed for the $^{93\text{m}}\text{Nb}$ x-ray peak, with a moving ^{137}Cs source to increase the count rate. The FWHM of the peaks remained unchanged. The fact that the slopes are similar at 17 keV and 122 keV

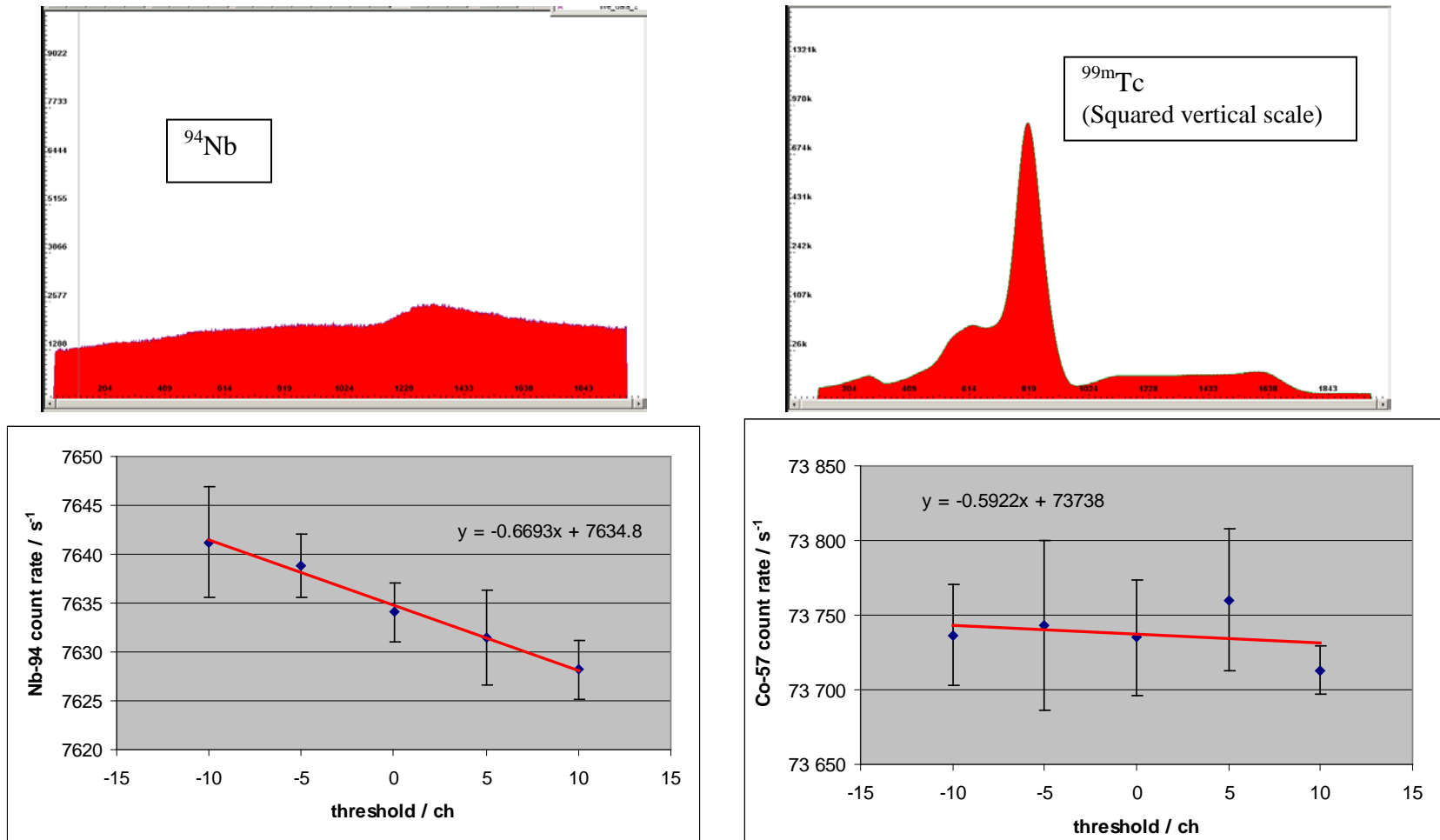


Figure 7. Energy spectrum measured with the SIRTl for ^{94}Nb and $^{99\text{m}}\text{Tc}$. The corresponding count rate sensitivity versus threshold position is shown below each spectrum. ^{57}Co has been used to simulate $^{99\text{m}}\text{Tc}$.

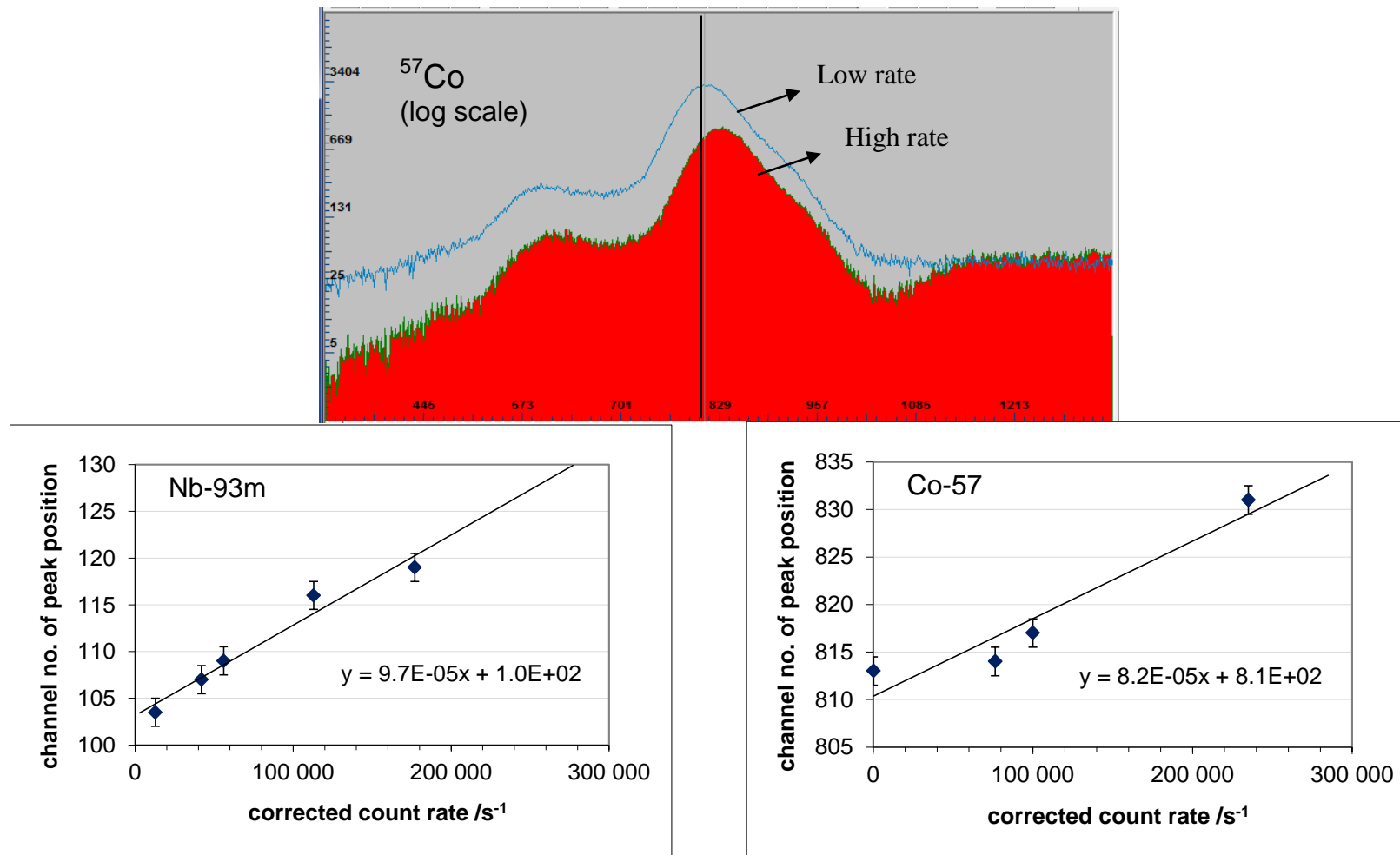


Figure 8. Top: ^{57}Co energy spectrum observed at low and high count rates showing the shift of the γ -ray peak. Bottom: Change of peak position versus the count rate corrected for live-time, for the $^{93\text{m}}\text{Nb}$ x-ray peak at 17 keV (left) and for the ^{57}Co γ -ray peak at 120 keV (right).

implies that there is a spectrum shift rather than a change in gain of the electronics. This is consistent with the fact that the SIRTl PMT has SbCs dynodes which are known to have a small rate effect. Consequently, the shift observed is probably related to a shift of the amplifier baseline which may be due to a slow phosphorescent component of the NaI(Tl) light (“afterglow” [9]). This seems consistent with the performance of the amplifier which, thanks to its baseline restorer circuitry, should remain stable at the level of 10^{-4} only at a low count rate (between 1000 s^{-1} and $50\,000 \text{ s}^{-1}$).

The stability of the whole electronic chain versus the count rate can also be checked by measuring a strong $^{99\text{m}}\text{Tc}$ source and looking for deviations from the exponential decay law. Figure 9 shows the SIRTl measurement results as a function of the $^{99\text{m}}\text{Tc}$ count rate in the detector. Each series of results has been renormalized to the KCRV in order to eliminate the influence of the $^{99\text{m}}\text{Tc}$ activity measurement by the NMI. The results, which are corrected for decay, should be constant but this is not the case and the deviation observed is identical for the two independent measurements of the NPL and LNE-LNHB ampoules. A relative effect of 1.8×10^{-3} is observed at $50\,000 \text{ s}^{-1}$. Decreasing A_E values corresponds to an increasing count rate (see equation (1)) and seems consistent with a shift of the energy spectrum towards high energy, assuming that the threshold position expressed in volts does not change. Indeed, similar to the ^{57}Co tests mentioned above, the 140 keV γ -ray peak position moved from channel 813 to channel 832 when the count rate increased from $38\,000 \text{ s}^{-1}$ to $120\,000 \text{ s}^{-1}$. Possible explanations for the decreasing A_E values versus the count rate are:

- a) Shift of the amplifier baseline: the shift of about 20 channels observed for the peak at 140 keV would correspond to a shift of 20 channels of the threshold position. However, Figure 7 shows that the measured count rate is not very sensitive to the threshold position for radionuclides such as ^{57}Co or $^{99\text{m}}\text{Tc}$ where most counts are in the photopeak. Consequently, a shift of the amplifier baseline is not sufficient to explain the observed decrease in A_E values.
- b) Pile-up between two below-the-threshold pulses: the rate of such pile-up events is of the order of the square of the count rate of below-the-threshold pulses multiplied by the width of these small pulses ($4 \mu\text{s}$). The count rate below the threshold can be estimated from PENELOPE Monte-Carlo simulations of 140.5 keV gamma-rays [12] as 10^{-3} of the total count rate. The pile-up rate at the maximum count rate of $2.5 \times 10^5 \text{ s}^{-1}$ is thus about 0.25 s^{-1} , which is negligible. Note: pile-up between one pulse above the threshold and any other pulse (below or above the threshold) would modify the measured energy spectrum but would have no influence on the count rate (corrected for dead time).
- c) Live-time correction: The MTR2 has been tested at the BIPM at count rates up to $44\,000 \text{ s}^{-1}$ [10] and at count rates of a few 10^5 s^{-1} at the LNE-LNHB and no significant bias in the live-time correction was observed. In addition, three MTR2 modules available at the BIPM were compared at a count rate of

$57\,000\text{ s}^{-1}$ and were found to agree within 2×10^{-5} , confirming that the MTR2 used for the SIRTI does not suffer any failure, bias or mis-adjustment.

In conclusion, although the influence of the count rate on the SIRTI response has been clearly observed, there is no explanation for the magnitude of the effect. Consequently, it was decided to limit the count rate in the comparison measurements to $20\,000\text{ s}^{-1}$ and use the exponential fit of Figure 9 to evaluate a type B uncertainty (see section 7).

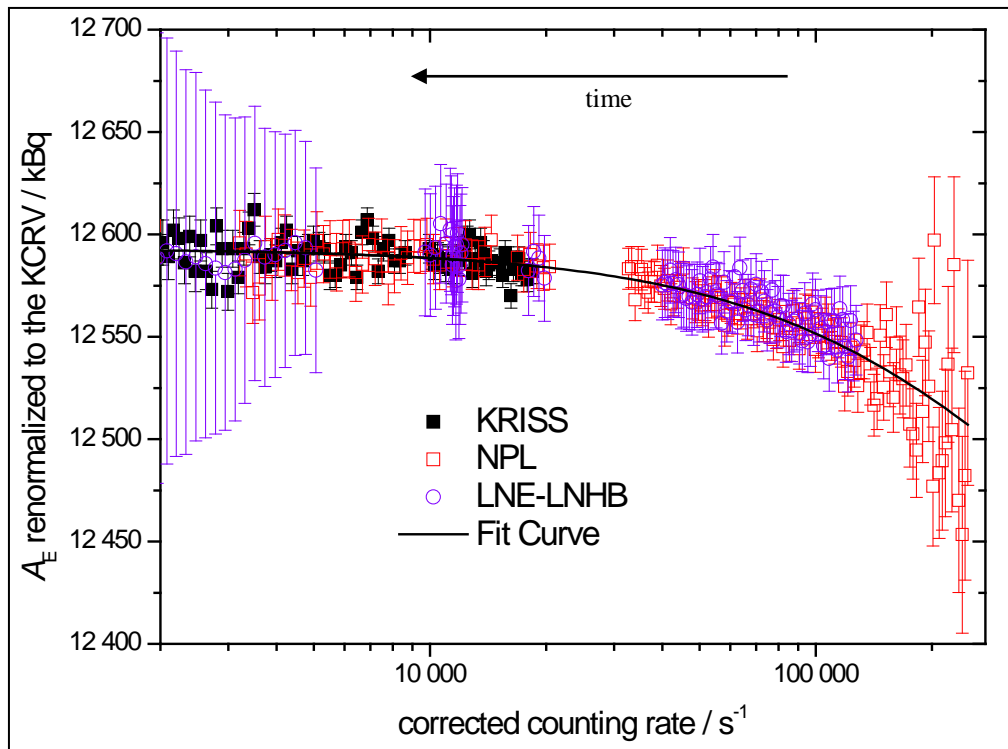


Figure 9. Normalized SIRTI equivalent activity for ^{99m}Tc as a function of the count rate. The line corresponds to an exponential fit. The large uncertainties on the left are due to a large ^{99}Mo impurity correction. See text.

4. Repeatability and reproducibility of the ^{94}Nb count rate above the threshold

The repeatability of the Nb measurement (the threshold setting in particular) has been measured at the BIPM under stable conditions over three days (temperature stable within 1°C and mean background rate of $75.70 (18)\text{ s}^{-1}$). Agreement within statistical uncertainty (2.7×10^{-4} in relative terms) has been obtained for the ^{94}Nb count rate above the threshold.

The reproducibility of SIRTI measurements has been measured using different sources (^{94}Nb , ^{57}Co , ^{134}Cs or ^{154}Eu) under changing measurement conditions as listed here:

- change of gain of the amplifier by 10 % followed by a re-adjustment of the threshold

- change of HV by 20 V followed by a re-adjustment of the threshold
- change of the MTR2 extending dead-time value (see Figure 5) and change of MTR2
- extension of the detector-to-amplifier cables
- slight changes of the position of the lead shielding and verticality of the detector
- change of surroundings (middle of the room or close to a lead wall)

All count rate measurements agreed within statistical uncertainty (5×10^{-4} in relative terms, at maximum).

As already mentioned, the response of a NaI(Tl) detector is known to be sensitive to temperature. However, each series of 10 Nb measurements of 700 s duration is preceded by a threshold setting to the $^{93\text{m}}\text{Nb}$ x-ray peak so that the Nb measurements made at different NMIs at temperatures ranging from 21 °C to 26 °C do not reveal any significant dependence on temperature (see Figure 10).

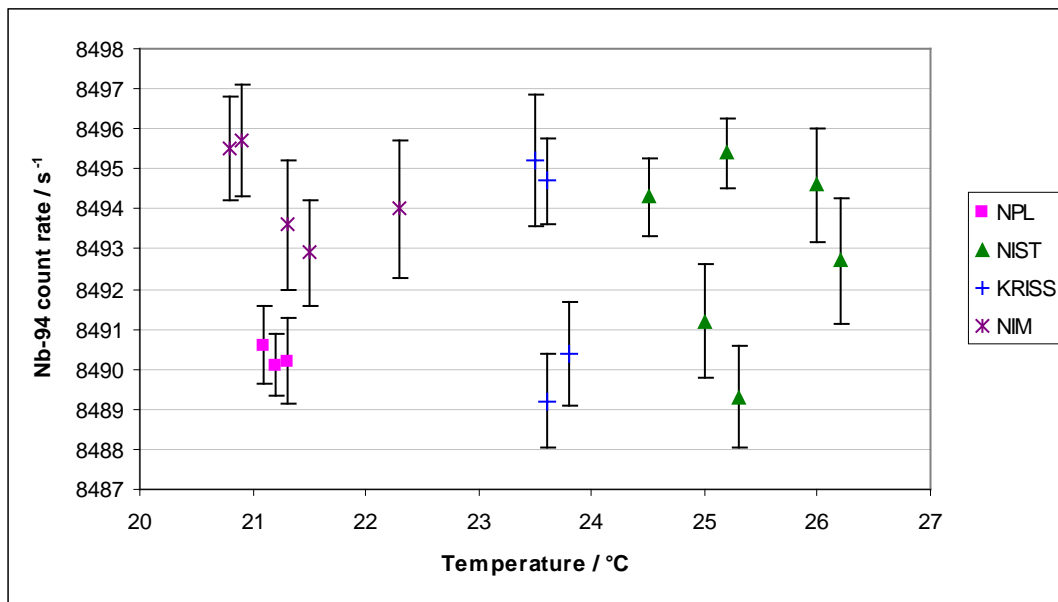
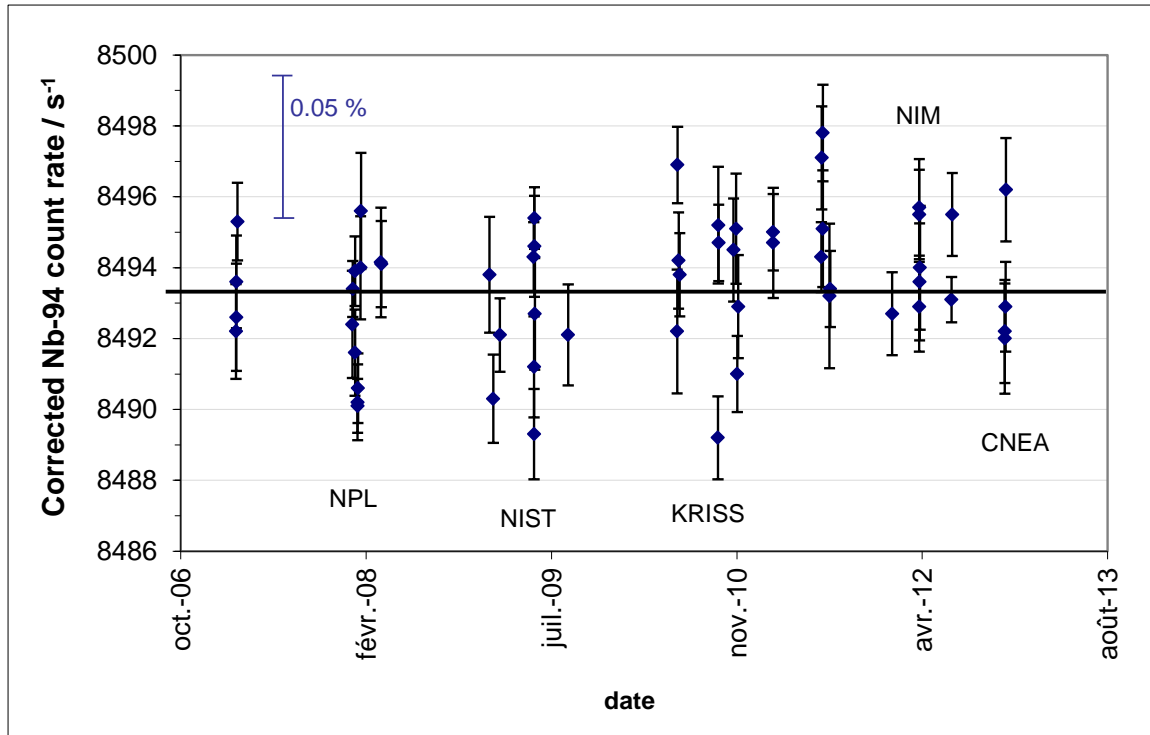


Figure 10. Reproducibility of the Nb measurements. The ^{94}Nb count rate above the threshold is independent of temperature.

The Nb measurement results are monitored over time in order to check the integrity of the detector following overseas travel. The results are corrected for decay and as a result of the very long half-life of ^{94}Nb , the uncertainty of the decay correction is negligible (and will remain so for at least the next 50 years). The results are plotted in Figure 11 which shows the long-term stability of the SIRTl. No significant trend is presently observed although the reduced chi-squared value is 2.7 showing that the quoted uncertainties are underestimated. The spread in the results should not be related to the threshold setting because it would correspond to errors of up to 7 channels in the threshold position and this is highly unlikely. The reason for this spread has not been identified and could be due to a combination of several effects. Consequently, the external standard uncertainty of the

weighted mean is used as an additional uncertainty component of the SIRTI ^{99m}Tc measurement uncertainty (see section 7).

A second Nb source, which always remains at the BIPM, is also monitored in order to determine the count rate ratio between the two sources and to allow replacement of the reference source in case of damage or loss.



diameter were observed, distributed in the cylindrical part and the head of the ampoule. The ampoule was centrifuged for 5 minutes at 3000 r/min to force the drops back into the ampoule base and a decrease in the measurement results A_E of 1.8×10^{-3} in relative terms was clearly observed (see Figure 13). Such an effect could be reproduced by Monte-Carlo simulations (see [12] for further details).

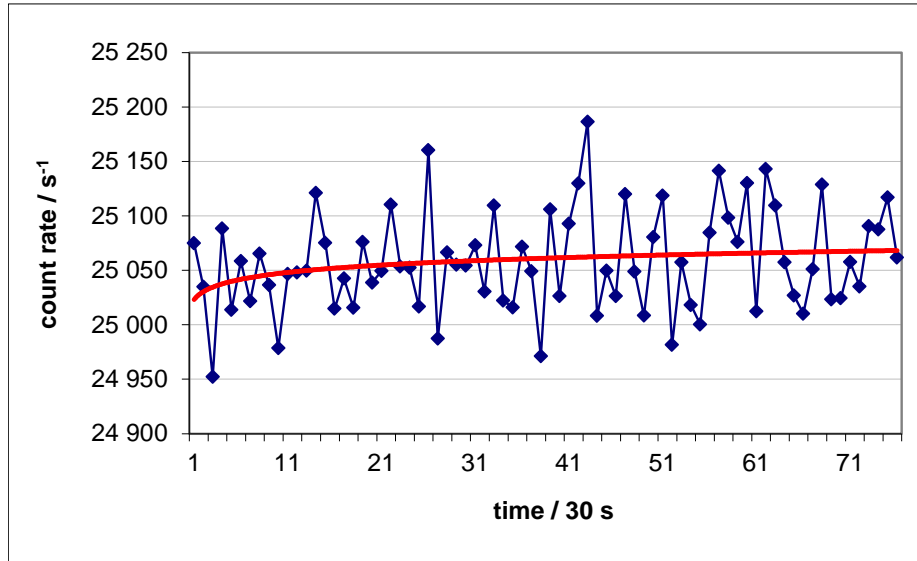


Figure 12. Measured count rate produced by an ampoule of ^{57}Co just after turning it upside-down. A 2×10^{-3} relative effect is observed in the first measurements.

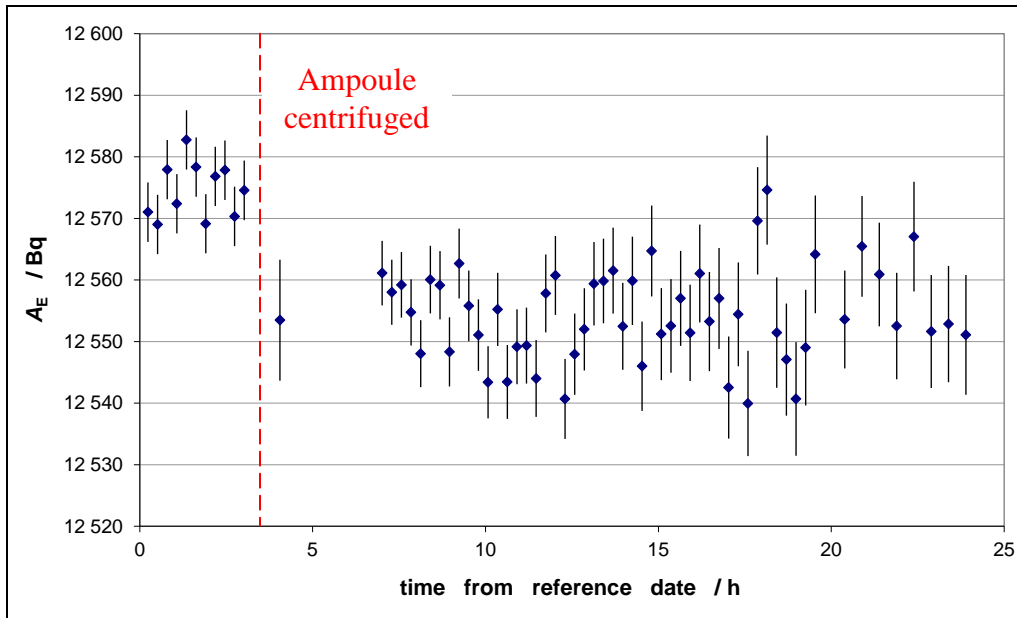


Figure 13. Change in SIRT measurement results A_E after centrifugation of the ampoule (NIST, 2009).

In order to avoid the formation of drops sticking to the inner walls, procedures for cleaning the ampoules before filling are applied by some NMIs and are based, for example, on dichlorodimethylsilane (ENEA) or on a siliconizing solution (KRISS).

6. Measurement procedure for ^{99m}Tc

The ^{99m}Tc measurements are preceded and followed by Nb and background measurements. In addition a background measurement is often made in-between two series of ^{99m}Tc measurements. The duration of each individual ^{99m}Tc measurement is limited in time because the decay during measurement may affect the live-time correction which assumes, in principle, a constant count rate. The effect of decay on the live-time correction has been studied by several authors in the past and a review of the subject was produced by R. Fitzgerald in 2009 [13]. This report is used to calculate the maximum duration of a measurement, depending on the count rate, such that the effect of the decay on the live-time correction is lower than 10^{-4} (see section 7).

7. Uncertainty evaluation of the ^{99m}Tc SIRTI measurements

The measurement model is given by (1). Because of the short half-life of ^{99m}Tc , the measured count rates cannot be averaged directly: the A_E value is calculated for each measurement individually and the law of propagation of uncertainty is applied to evaluate $u(A_E)$ for each measurement. The weighted mean result of all the ^{99m}Tc measurements is then calculated and the uncertainty of the mean is evaluated taking into account the correlation between all the A_E measurements due to the ^{99m}Tc half-life, the background rate and the ^{99}Mo activity, if present, in the solution (see GUM F.1.2.3 [14]).

A typical uncertainty budget of a SIRTI measurement result A_E is given in Table 3.

The uncertainty contribution due to the SIRTI drift at a high count rate is obtained by calculating the mean count rate over the ^{99m}Tc series of measurements and deducing the corresponding mean drift of the SIRTI using the exponential curve shown in Figure 9.

The influence of the density and volume of the radioactive solution as well as of the geometry of the glass ampoule has been investigated using a Monte Carlo method with PENELOPE 2008. The results are indicated in Table 3 and will be presented in another report [12].

As explained in section 5, drops of solution sticking to the inner walls of the ampoule are a source of uncertainty. In many cases, the drops are small and mainly situated on the cylindrical part of the ampoule. In such cases, the effect on the ^{99m}Tc measurement was shown to be negligible by Monte-Carlo simulations [12]. If larger drops are observed and placed in the ampoule head, the effect can be in the order of a few 10^{-3} . This uncertainty reduces to zero if the ampoule is centrifuged.

	Uncertainty contributions due to	Relative standard uncertainties $\times 10^4$	Comments	Evaluation method
1	^{99m}Tc measurement ratio including live-time, background, decay corrections	1 to 20	Standard uncertainty of the weighted mean taking into account the correlation due to the ^{99m}Tc half-life, background and ^{99}Mo impurity	A
2	Nb reference source measurements	1	Standard uncertainty of the weighted mean	A
3	Long-term stability/reproducibility of the SIRTI	0.3	Standard uncertainty of the weighted mean of all Nb measurements since 2007	A
4	Effect of decay on the live-time correction	< 1	Maximum measurement duration evaluated from [13]	B
5	SIRTI drift at high count rate	2 to 4	Mean possible drift; depending on the activity of the ^{99m}Tc source	B
6	Ampoule dimensions	7	Evaluated by Monte-Carlo simulation [12]	B
7	Ampoule filling height	6		B
8	Solution density	0.8		B
9	Drops on the walls of the ampoule	0 to 20		B
11	^{99m}Tc activity	40 to 110	From the NMI	B

Table 3. Typical uncertainty budget of a SIRTI A_E measurement for ^{99m}Tc

A decrease of the A_E measurements versus time is occasionally observed, which can be resolved by adjusting the activity of ^{99}Mo impurity in the solution. An additional type B uncertainty is then evaluated by looking at the effect of this adjustment on the weighted mean A_E result.

In the BIPM.RI(II)-K4.Tc-99m comparisons carried out to date using the SIRTI, the combined standard uncertainty related to the SIRTI measurements is typically 11×10^{-4} , in relative terms. This contribution is small compared to the relative uncertainty of the NMI $^{99\text{m}}\text{Tc}$ standardization which is, at the best, 40×10^{-4} .

Finally, the BIPM.RI(II)-K4.Tc-99m comparison is linked to the SIR (BIPM.RI(II)-K1.Tc-99m) by the measurement of two independent $^{99\text{m}}\text{Tc}$ solutions (from the LNE-LNHB and the NPL) in both systems [5]. Each SIRTI A_E comparison result is then multiplied by the linking factor in order to compare the SIRTI results with the SIR results obtained by NMIs that are located close to the BIPM geographically. This introduces an additional relative uncertainty due to the linking factor of 16×10^{-4} . Results of the SIRTI comparison are published in the key comparison data base of the CIPM MRA [15].

The extension of the SIRTI to other radionuclides such as ^{18}F is in preparation.

Conclusion

The transfer instrument of the SIR was established at the BIPM to enable world-wide activity comparisons of short-lived radionuclides like those used in nuclear medicine. This report describes the SIRTI in detail, i.e. the detector, the mechanical parts and the associated electronics) and shows the results of the tests made during its development.

The sensitivity of the ^{94}Nb measurements to the threshold position is such that each measurement should be preceded by a threshold setting using the $^{93\text{m}}\text{Nb}$ x-ray peak. The reproducibility of the ^{94}Nb measurements shows larger fluctuations than expected in view of the stated uncertainty, but remains sufficiently small to have little influence on the SIRTI measurement results.

The count rate in the SIRTI measurements needs to be limited to $20\,000\text{ s}^{-1}$ because of a drift of the system observed at high count rate.

Care should be taken to avoid drops of solution sticking to the inner wall of the head of the ampoule, which could have a relative effect on the $^{99\text{m}}\text{Tc}$ measurement results of a few 10^{-3} .

The uncertainty contribution of the SIRTI in a $^{99\text{m}}\text{Tc}$ comparison is typically 11×10^{-4} , in relative terms, to which the uncertainty of the NMI standardization should be added as well as the relative uncertainty of 16×10^{-4} of the link to the BIPM.RI(II)-K1.Tc-99m comparison (SIR).

Acknowledgements

The authors would like to thank R. Fitzgerald, Y. Hino, L. Johansson, S. Pommé, M. Unterweger, A. Yunoki, P. Allisy and G. Ratel for their support in the framework of the TIWG(II) of the CCRI(II). The BIPM is indebted to the LNE-LNHB for the donation of the MTR2 and to the IRMM for the donation of the Nb reference sources. Last but not least, the workshop of the BIPM is thanked for machining the detector tripod, the lead shielding and source holders.

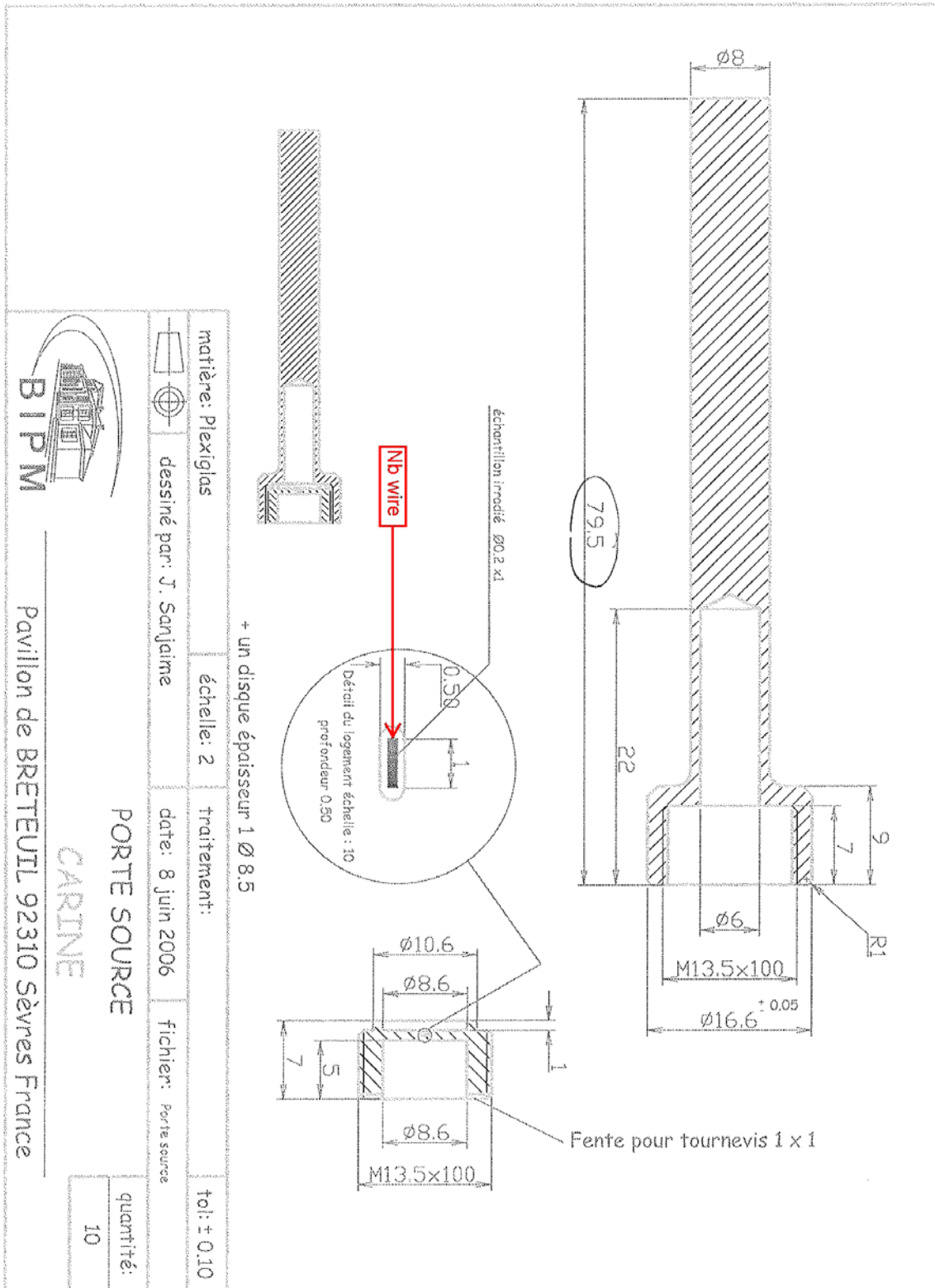
References

- [1] Reher D. and Allisy P., 2005, Proposal for a travelling well detector (TWD) for CCRI(II) key comparisons of short lived radionuclides, CCRI(II) working document CCRI(II)/05-08.
- [2] Remit of the CCRI(II) Transfer Instrument Working Group, 2009, CCRI(II)/09-15.
- [3] CCRI(II) Transfer Instrument Working Group, 2005, report of the meeting on 4 November at the BIPM, TIWG(II)/05-05.
- [4] NUDAT2.5, [National Nuclear Data Center](#), Brookhaven National Laboratory, based on ENSDF and the Nuclear Wallet Cards.
- [5] Michotte C. *et al.*, Calibration of the new SIRTl against the SIR for ^{99m}Tc , in preparation.
- [6] Bouchard J., 2000, MTR2: a discriminator and dead-time module used in counting systems, [Appl. Radiat. Isot.](#) **52**, 441-446.
- [7] Chauvenet B. *et al.*, 1987, Measurements of high-activity sources with a $4\pi\beta\text{-}\gamma$ coincidence system, [Nucl. Instr. and Meth. A](#) **259**, 550-556.
- [8] Baerg A.P. *et al.*, 1976, Live-Timed Anti-Coincidence Counting with Extending Dead-Time Circuitry, [Metrologia](#) **12**, 77-80.
- [9] Knoll G.F., 1979, Radiation Detection and Measurement, Wiley, New York, p. 258 and 293.
- [10] Michotte C., Nonis M., 2009, Experimental comparison of different dead-time correction techniques in single-channel counting experiments, [Nucl. Instr. and Meth. A](#), **608(1)**, 163-168.
- [11] Michotte C., Fitzgerald R., 2010, Activity measurements of the radionuclide ^{99m}Tc for the NIST, USA, in the ongoing comparison BIPM.RI(II)-K4.Tc-99m, [Metrologia](#) **47**, *Tech. Suppl.*, 06027.
- [12] Michotte C. *et al.*, Monte-Carlo simulations of the SIRTl for ^{99m}Tc and ^{18}F , in preparation.
- [13] Fitzgerald R., 2009, The combined dead-time and decay effect on live-timed counting systems with fixed, extending dead times. Transfer Instrument Working Group of the CCRI(II), Document TIWG(II)/09-10.
- [14] BIPM, IEC, IFCC, ILAC, ISO, IUPAC, IUPAP and OIML, 2008 Evaluation of measurement data — Guide to the expression of uncertainty in measurement, Joint Committee for Guides in Metrology, JCGM 100:2008, GUM 1995 with minor

corrections, http://www.bipm.org/utis/common/documents/jcgm/JCGM_100_2008_E.pdf

- [15] CIPM MRA: *Mutual recognition of national measurement standards and of calibration and measurement certificates issued by national metrology institutes*, International Committee for Weights and Measures, 1999, 45 pp. <http://www.bipm.org/en/cipm-mra/>.

Annex 1. The plastic holder of the Nb reference source



Annex 2. The brass liner of the SIRT1

